2

# Application of finite element analysis in dentistry

Ming-Lun Hsu and Chih-Ling Chang
*Department of Dentistry, National Yang-Ming University*
*Taipei, Taiwan*

## 1. Introduction

Since Brånemark introduced the concept of osseointegration and the possibility of anchoring dental prostheses by intraosseous implantation in 1969, the clinical use of implants for oral and maxillofacial rehabilitation has rapidly expanded over the past 20 years. Biomechanical factors play a substantial role in implant success or failure. The application of occlusal forces induces stresses and strains within the implant-prosthesis complex and affects the bone remodeling process around implants.To achieve optimized biomechanical conditions for implant-supported prostheses, conscientious consideration of the biomechanical factors that influence prosthesis success is essential.

Many different methods have been used to study the stress/strains in bone and dental implants. Photoelasticity provides good qualitative information pertaining to the overall location of stresses but only limited quantitative information. Strain-gauge measurements provide accurate data regarding strains only at the specific location of the gauge. Finite element analysis (FEA) is capable of providing detailed quantitative data at any location within mathematical model. Thus FEA has become a valuable analytical tool in the assessment of implant systems in dentistry.

## 2. Assumptions in the use of FEA in the implant-bone biomechanical system

The power of the FEA resides principally in its versatility and can be applied to various physical problems. The structure analyzed can have arbitrary shape, loads, and supporting conditions, furthermore, the mesh can mix elements of different types, shapes, and physical properties. This great versatility is contained within a single computer program and the selection of program type, geometry, boundary conditions, element selection are controlled by user-prepared input data. The principal difficulty in simulating the mechanical behavior of dental implants lies in the modeling of human maxilla and mandible and its response to applied load. Certain assumptions are needed to make the modeling and solving process possible and these involve many factors which will potentially influence the accuracy of the FEA results: (1) detailed geometry of the implant and surrounding bone to be modeled, (2) boundary conditions, (3) material properties, (4) loading conditions, (5) interface between bone and implant, (6) convergence test, (7) validation.

## 3. Geometry

The attractive feature of finite element is the close physical resemblance between the actual structure and its finite element model. Excessive simplifications in geometry will inevitably result in considerable inaccuracy. The model is not simply an abstraction; therefore, experience and good engineering judgment are needed to define a good model. Whether to perform a two-dimensional (2-D) or three-dimensional (3-D) finite element model for the study is a significant query in FEA. It is usually suggested that, when comparing the qualitative results of one case with respect to another, a 2-D model is efficient and just as accurate as a 3-D model; although the time needed to create finite element models is decreasing with advanced computer technology, there is still a justified time and cost savings when using a 2-D model over 3-D, when appropriated. However, 2-D models cannot simulate the 3-D complexity within structures, and as a result are of little clinical values. The group of 3-D regional FE models is by far the largest category of mandible related researches. This is because modeling only the selected segment of mandible is much easier than modeling the complete mandible. In many of these regional models, reproduced boundary conditions are often oversimplified, and yield too much significance to their predictive, quantitative outcome.

When a model is supposed to be 2-D, the z axis (third dimension) must be specified to have either a plane-strain or a plane-stress condition. Plane strain assumes the model to be infinitely thick, so no strain occurs but some stress will progress in the z direction. Plane stress supposes the model to be thin enough, so no stress occurs but it has some strain in the z direction. In 3-D analysis, the stress and strain condition can be evaluated in all three axes (x, y, and z). The first step in FEA modeling is to represent the geometry of interest in the computer. In some 2-D FEA studies, the bone was modeled as a simplified rectangular configuration with the implant (Fig.1). The mandible was treated as an arch with rectangular section or a simplified segment as cancellous core surrounded by a 1.3-mm cortical layer with the overall dimensions of this block were 23.4 mm in height, 25.6 mm in mesiodistal length, and 9.0 mm in buccolingual width in 3-D FEA models (Fig.2). A dried specimen was scanned and imported into image analysis software (Image Tool 1.21; UTHSC, San Antonio, Tex, U.S.A.) to create the digital image of a sagittal cut of the palatine process of the 2-D maxilla. The outline of the image was manually plotted and each point converted into x and y coordinates. The coordinates were finally imported into the ANSYS software as keypoints of the definitive image. The same procedure was used to create the implant image (Fig.3). Computerized tomographic images of a human edentulous maxillary first molar area exhibiting buccal bone irregularities were acquired. The maxilla was approximately 11 mm in width bucco-lingually and 13 mm in height infero-superiorly. The cross-sectional image was then extruded to create a three-dimensional section of maxilla 6.5 mm in length in the mesio-distal direction. Due to symmetry with respect to the bucco-lingual plane in the geometry and loading, only half of the FE model needed to be considered (Fig.4).With the development of digital imaging techniques recently, more efficient methods are available included the application of specialized software for the direct transformation of 2- or 3-D information in image data from computed tomography (CT) or magnetic resonance imaging (MRI) into FEA meshes. Solid models of a mandibular segment, crown, and dental implants were constructed using the computer-aided design (CAD) system (Pro-Engineering, PTC, New York, NY, U.S.A.) to create 3-D FE models from the data basis originally stemmed from CT images. The need for accurate FE models of the complete mandible (Fig.5) in realistic simulation is becoming more acknowledged to evaluate an optimal biomechanical distribution of stresses in mandibular implant-supported fixed restorations both at the level of the prosthetic superstructure and at the level of the implant infrastructure.

## 4. Material Properties

Material properties greatly influence the stress and strain distribution in a structure. These properties can be modeled in FEA as isotropic, transversely isotropic, orthotropic, and anisotropic. The properties are the same in all directions, therefore, only two independent material constants of Young's modulus and Poisson's ratio exist in an isotropic material. In most reported studies, an assumption was made that the materials were homogenous and linearly isotropic. How to determine the complex cancellous pattern was very tough, so the cancellous bone network ignored in early FEA studies. Therefore, it was assumed that cancellous bone has a solid design inside the inner cortical bone shell. There are several methods to determine the physical properties of bone, such as tensile, compressive, bending, and torsion testing, pure shear tests, micro- and nano-indentation tests, acoustic tests, and back-calculation using FE models (Table1). The values 13.7 GPa and 1.37 GPa have been frequently used for the Young's modulus of cortical and cancellous bone, respectively. The original source for those values is a compressive test study on human vertebrae. However, compressive tests are subject to the confounding factors of proper specimen alignment and compliance of the loading fixture, which are not factors in ultrasonic pulse technique. Consequently, in the current study, cortical and cancellous bone were given a Young's modulus of 20.7 GPa and 14.8 GPa, respectively, according to the ultrasound study by Rho et al. Poisson's ratio were assumed to be 0.3 for both cortical and cancellous bone. Several studies incorporated simplified transversely isotropy (Table2) instead of orthotropy into their FE models demonstrated the significance of using anisotropy (transversely isotropy) on bone-implant interface stresses and peri-implant principal strains. It was concluded that anisotropy increased what were already high levels of stress and strain in the isotropic case by 20-30% in the cortical crest. In cancellous bone, anisotropy increased what were relatively low levels of interface stress in the isotropic case by three- to four folds. To incorporate more realistic anisotropic materials for bone tissues in maxilla or mandible, the FE model may employ fully orthotropy for compact bone and transversely isotropy for cancellous bone (Table 3), since they are currently available material property measurements of human mandible. Because of material properties for human maxillary bone were not available, this may influence the accuracy and applicability of the study results. However, by assigning fully orthotropic material to compact bone, the high quality anisotropic FE model of the segmental maxilla may bring us one important step closer toward realizing realistic maxilla related simulation. An orthotropic material has three planes of mirror symmetry and nine independent constants as compared to one axis of symmetry and five independent constants for transverse isotropy. Orthotropy is not in itself a problem for the finite element method. However, the cross-sectional shape of the mandible does not easily lend itself to the use of orthotropic material properties, for which the symmetry axes would presumably change from point to point, following the irregular elliptical shape of the mandibular cross section. A transversely isotropic material behaves identically in all planes perpendicular to the axis of symmetry. The unique symmetry axis for compact bone was along the mesio-distal direction with the bucco-lingual plane being a plane of elastic isotropy. The unique symmetry axis for cancellous bone of the edentulous mandible was in the infero-superior direction with the anatomic transverse plane being a plane of elastic isotropy.

## 5. Boundary Conditions

Zero displacement constraints must be placed on some boundaries of the model to ensure an equilibrium solution. The constraints should be placed on nodes that are far away from the region of interest to prevent the stress or strain fields associated with reaction forces from overlapping with the bone-implant interface. In the maxillary FEA models, the nodes along the external lines of the cortical bone of oral and nasopharyngeal cavities were fixed in all directions (Fig.3). Most FEA studies modeling the mandible set the boundary condition was constrained in all directions at the nodes on mesial and distal borders.

Since only half of the model was meshed, symmetry boundary conditions were prescribed at the nodes on the symmetry plane. Models were constrained in all directions at the nodes on the mesial bone surface. Because of symmetry conditions, these constraints were also reproduced on the distal bone surface (Fig.6).

An individual geometry of the complete range of mandible was created, meanwhile the functions of the mastication muscles, ligaments and functional movement of temporomandibular joints simulated. The boundary conditions included constraining all three degrees of freedom at each of the nodes located at the joint surface of the condyles and the attachment regions of the masticatory muscles (masseter, temporalis, medial pterygoid, and lateral pterygoid) (Fig.7). Expanding the domain of the model can reduce the effect of inaccurate modeling of the boundary conditions. This, however, is at the expense of computing and modeling time. Modeling a 3-D mandibular model at distances greater that 4.2 mm mesially or distally from the implant did not result in any significant further yield in FEA accuracy.

## 6. Loading Conditions

Mastication involves a repeated pattern of cyclic impacts that causes loading to the implant components and distributes the force to the bone interface. When applying FE analysis to dental implants, it is important to consider not only axial loads and horizontal forces (moment-causing loads) but also a combined load (oblique occlusal force) because the latter represents more realistic masticatory pattern and will generate considerable localized stresses in compact bone. Bite force studies indicated considerable variation from one area of the mouth to another and from one individual to the next. In the premolar region, reported values of maximal bite force range from 181-608 N. Average forces of more than 800 N for male young adults and 600 N for female young adults have been recorded in the molar region. Small forces of 290 and 240 N, respectively, have been measured in the incisal region. The variation may be related to many factors, such as muscle size, bone shape, sex, age, degree of edentulism, and parafunction. In the maxillary anterior region, the occlusal force was assumed to be 178 N could not impair osseointegration or induce bone resorption may be appropriate (Fig.8). A 200-N vertical and a 40-N horizontal load were applied to the occlusal surface of the crown (Fig.9). These loads represent average means recorded on patients with endosseous implants. It should be noted that a great spectra of vertical loads/forces have been reported for patients with endosseous implants (means range :

91-284 N), and the loads appear to be related to the location of the implant, as well as to food consistency. In the previous studies, the locations for the force application were specifically described as cusp tip, distal fossa, and mesial fossa. When occlusal forces exerted from the masticatory muscles, the buccal functional cusps of the mandibular teeth will be forced to contact with central, distal, and mesial fossa. Hence, bite force applied to the occlusal surface of the crown may be more reasonable than the abutment of the implant.

## 7. Bone-implant interface

Analyzing force transfer at the bone-implant interface is an essential step in the overall analysis of loading, which determines the success or failure of an implant. It has long been recognized that both implant and bone should be stressed within a certain range for physiologic homeostasis. Overload can lead to bone resorption or fatigue failure of the implant, whereas underloading of the bone may cause disuse atrophy and subsequent bone loss. Most FEA models, the bone-implant interface was assumed to be perfect, simulating 100% osseointegration. This does not occur so exactly in clinical situations. Up until recently, linear static models have been employed extensively in finite element studies of dental implants. However, the validity of a linear static analysis is questionable for more realistic situations such as immediate loading.

Currently FEA programs provide several types of contact algorithms for simulation of contacts. Three different contact types defined in ANSYS—"bonded", "no separation", and "frictionless"—are used to describe the integration quality at the implant-compact bone interface. The "bonded" type simulates perfect osseointegration in which the implant and the surrounding compact bone are fully integrated so that neither sliding nor separation in the implant-bone interface is possible. The "no separation" type indicates an imperfect osseointegration in which separation at the contact interface is not allowed but frictionless sliding between the implant and compact bone may take place. The poorest osseointegration is modeled by a standard unilateral "frictionless" contact, which implies that a gap between the implant and the peri-implant compact bone may exist under an occlusal force. To obtain initial stability for the situation of immediate loading after implantation, it was modeled using nonlinear frictional contact elements, which allowed minor displacements between implant and bone. Under these conditions, the contact zone transfers pressure and tangential forces (i.e., friction), but no tension. The friction coefficient was set to 0.3. The friction between contact surfaces can also be modeled with contact algorithms. Ding's study was modeled using nonlinear frictional contact elements, which allow minor displacements between implant and bone to keep the implant stable and provide an excellent simulation of the implant–bone interface with immediate load.

## 8. Convergence Test

The p-element method in ANSYS was used for the convergence tests, and by this method the polynomial level (p-level) of the element shape functions was manipulated. This differs from the more traditional h-method in which the mesh must be refined to obtain a suitable convergence in displacement or stress results (Fig.10). It is difficult to obtain a suitable mesh of a 3-D object with irregular shaped volumes and refining such a mesh in a consistent manner to ensure convergence is a cumbersome process. By contrast, once a suitable mesh is constructed in the p-method, it is kept unchanged while the polynomial level is increased from two to as high as eight until convergence is obtained. When an iterative solution method was used with a starting p-value of two and a tolerance of 1% for convergence checking, the analysis was considered to have converged if the global strain energy changed by less than 1%. Changing of the global strain energy was required to be less than 5% at a p-level of four at convergence could be also considered to have converged.

## 9. Validation

To validate the FE model, Sekine and coworkers measured the labiolingual mobility of 41 isolated osseointegrated implants in 8 human mandibles clinically using a displacement -measuring lever with electric strain gauges. The measuring point was 6 mm from the margin of bone shown on standardized x-rays of each implant. The load was increased linearly up to 20 N and observed implant displacement was 17 to 58 μm. The results of the FEA model could be compared with a real clinical situation, a similar load applied to the test implant in the study. This means that result of the FEA was similar to the clinical situation, thus the FE model was valid. The resulting level of implant displacement of Hsu's study was 17μm for a high-density model and 19μm for a low density bone model which revealed the calculated load-displacement values were close to values reported for osseointegrated implants in vivo. Therefore, an in vivo experiment could be conducted to verify the FEA results.

## 10. Statistical analysis

Statistical analysis has seldom been used in FEA. However, Hsu et al used a pair-wise t-test in his study to analyze results obtained from FE model. In this manuscript biomechanical performance of endodontically treated teeth restored with three post materials in three different length of post were evaluated with a 3-D FE model. The choice of the applicable stress representation criterion was based on an evaluation of the failure predictive potential of the analysis performed. The von Mises energetic criterion was then chosen as a better representative of a multiaxial stress state. These evaluations were carried out in three regions and 25 equally spaced points were sampled for plotting various pattern graphics as well as conducting statistical tests. A pair-wise t-test was applied to evaluate the difference among different groups. Statistical analysis was utilized properly to enrich the result and make the FEA meaningful.

## 11. Conclusion

With rapid improvements and developments of computer technology, the FEA has become a powerful technique in dental implant biomechanics because of its versatility in calculating stress distributions within complex structures. By understanding the basic theory, method, application, and limitations of FEA in implant dentistry, the clinician will be better equipped to interpret results of FEA studies and extrapolate these results to clinical situations. Thus, it is a helpful tool to evaluate the influence of model parameter variations once a basic model is correctly defined. Further research should focus in analyzing stress distributions under dynamic loading conditions of mastication, which would better mimic the actual clinical situation.

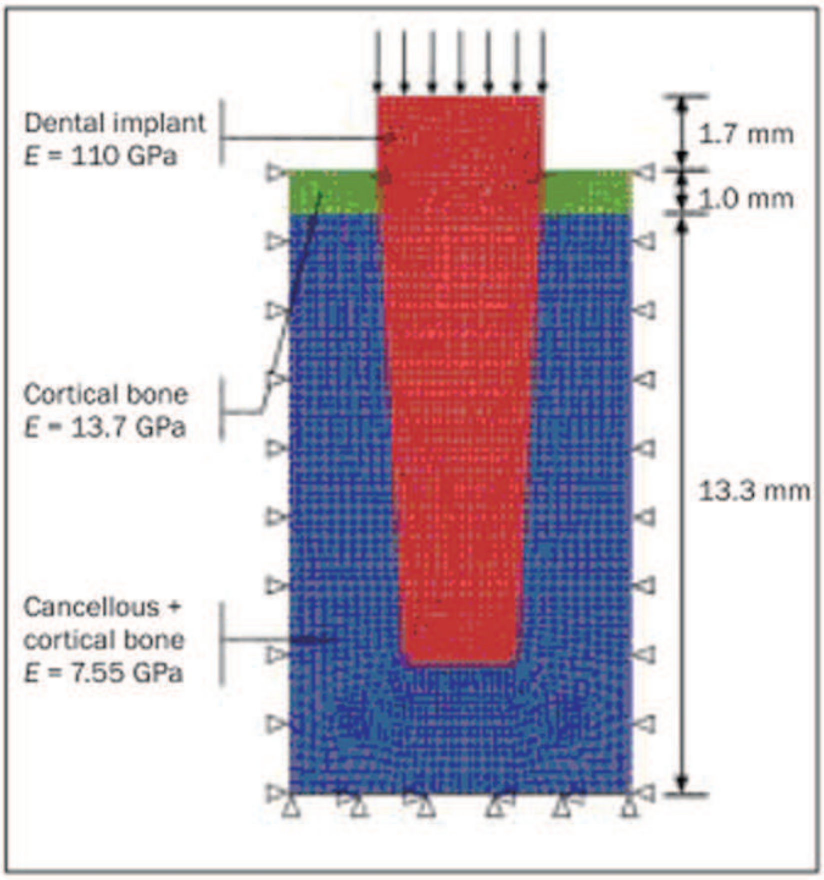


Fig. 1. The bone was modeled as a simplified rectangular configuration with the implant in 2-D FEA model (Courtesy from Shi L. et al. Int J Oral Maxillofac Implants 2007).

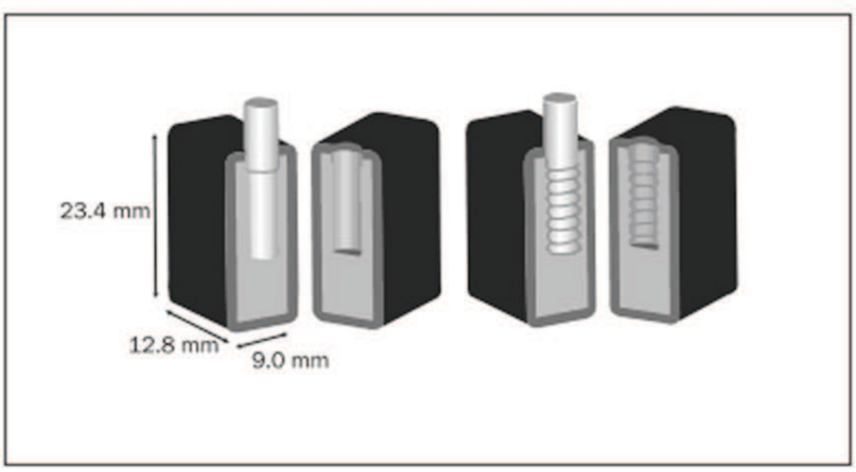


Fig. 2. The mandible was treated as a simplified segment as cancellous core surrounded by a 1.3-mm cortical layer with the overall dimensions of this block were 23.4 mm in height, 25.6 mm in mesiodistal length, and 9.0 mm in buccolingual width in 3-D FEA models (Courtesy from Tada S. et al. Int J Oral Maxillofac Implants 2003).

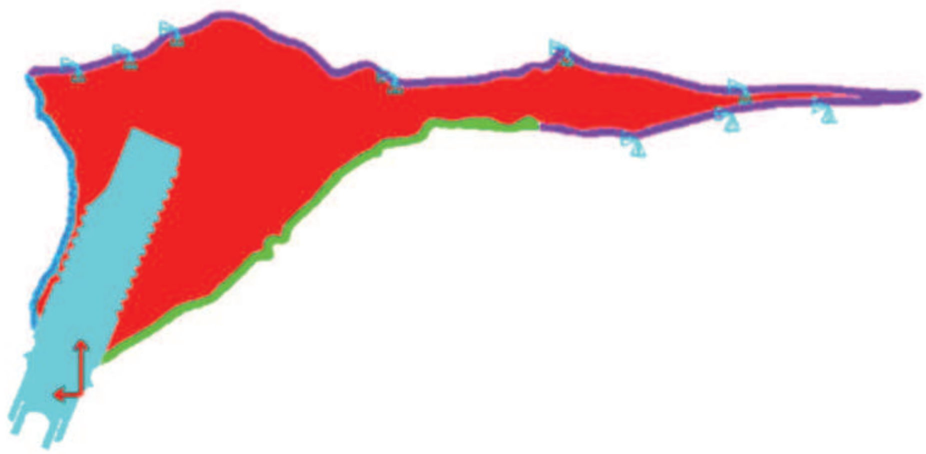

Fig. 3. The outline of the digital image was manually plotted and each point converted into x and y coordinates. The coordinates were finally imported into the ANSYS software as keypoints of the definitive image of the 2-D maxilla with implant (Courtesy from Saab XE et al. J Prosthet Dent 2007).

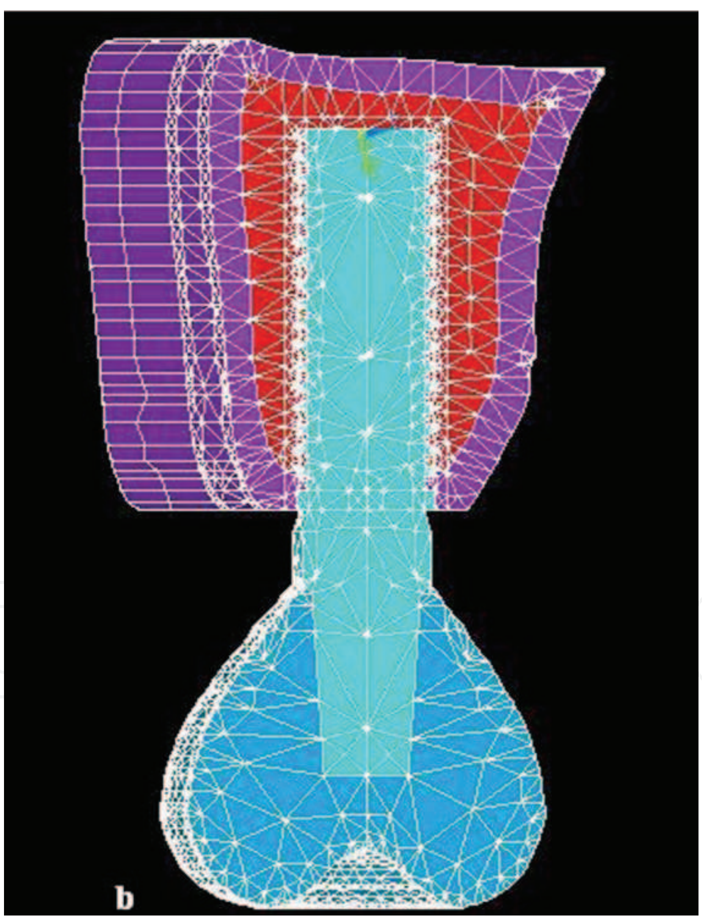


Fig. 4. Cross-sectional view on the symmetry plane of the meshed models with the implant embedded in the maxillary right first molar area and a gold alloy crown with 2-mm occlusal thickness was applied over the titanium abutment.

Fig. 5. A complete range of mandible reconstruction from CT and implants embedded in the posterior zone (Courtesy from Liao SH et al. Comput Med Imaging Graph 2008).

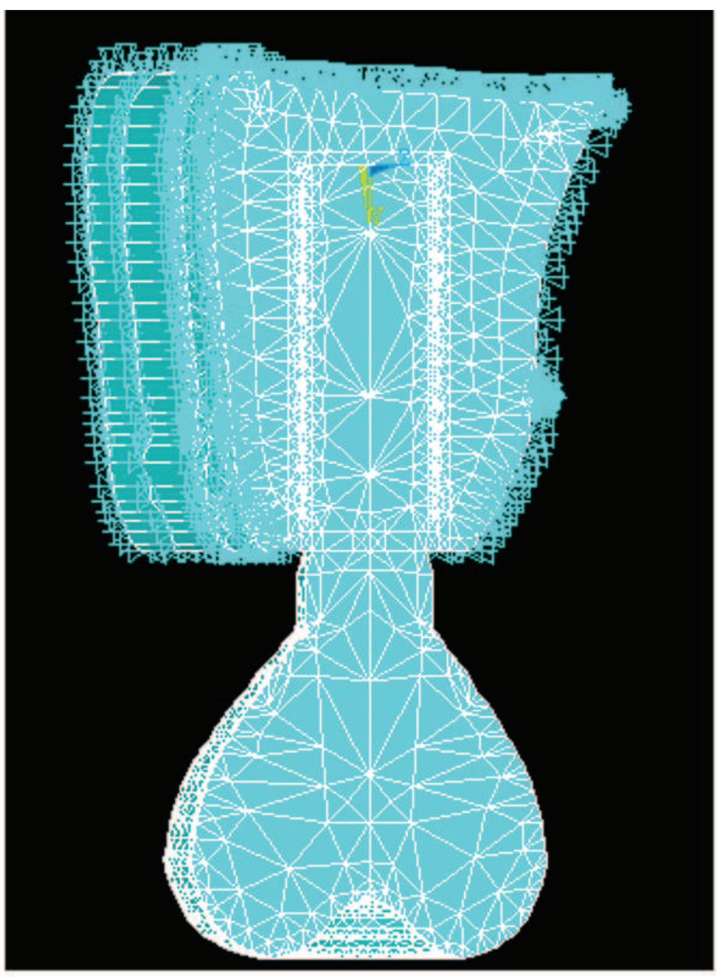

Fig. 6. Symmetry boundary conditions were prescribed at the nodes on the symmetry plane and the models were constrained in all directions at the nodes on the mesial and distal bone surface.

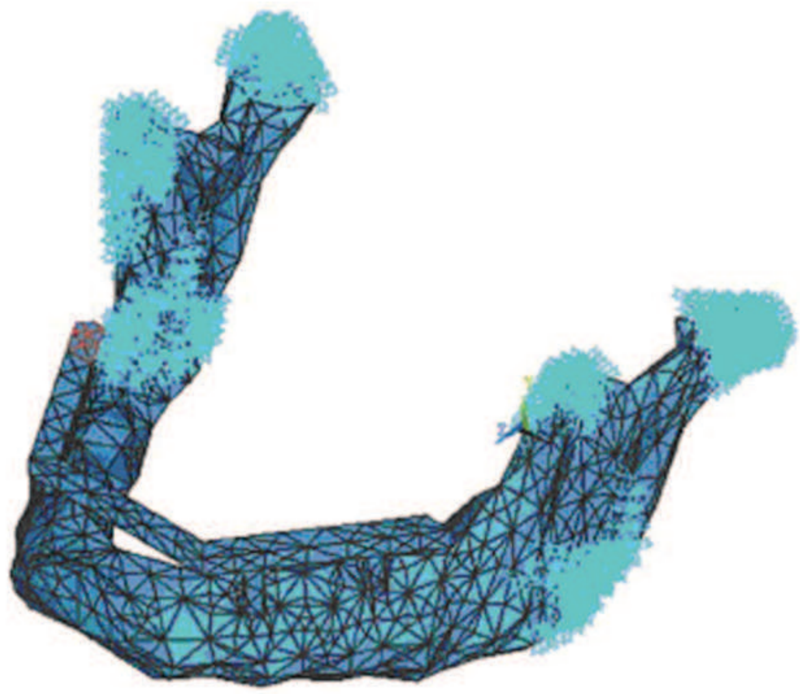

Fig. 7. All three degrees of freedom at each of the nodes located at the joint surface of the condyles and the attachment regions of the masticatory muscles (masseter, temporalis, medial pterygoid, and lateral pterygoid) were constrained (Courtesy from Nagasao T. et al. J Craniomaxillofac Surg 2002).

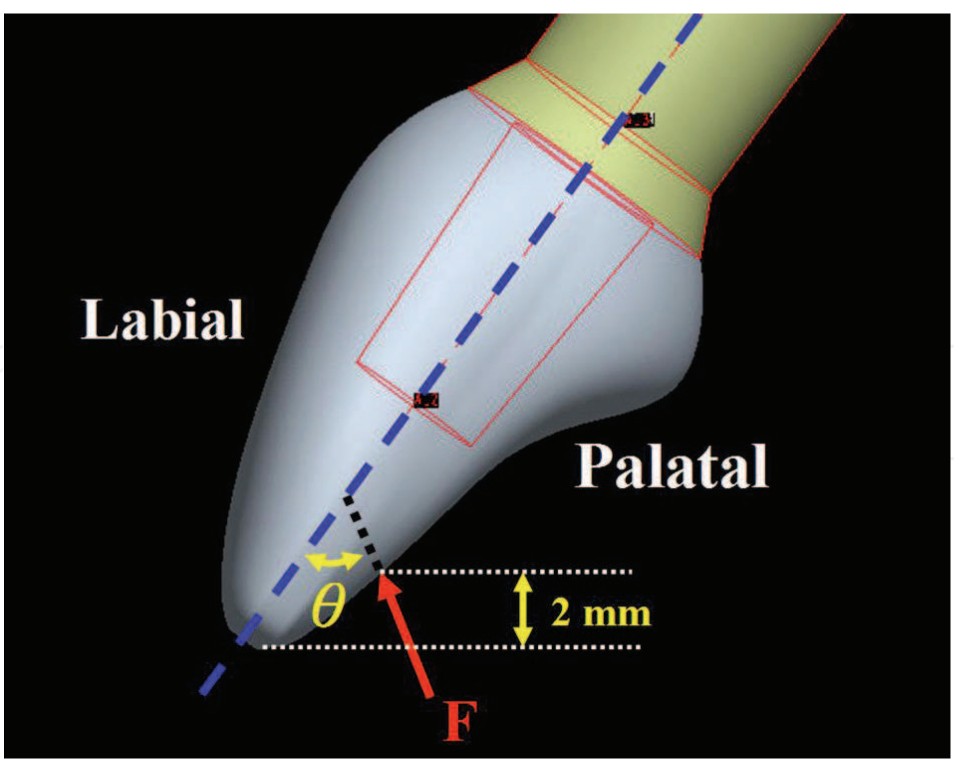


Fig. 8. In the maxillary anterior region, an occlusal load (F) of 178 N was applied on a node at the crown.

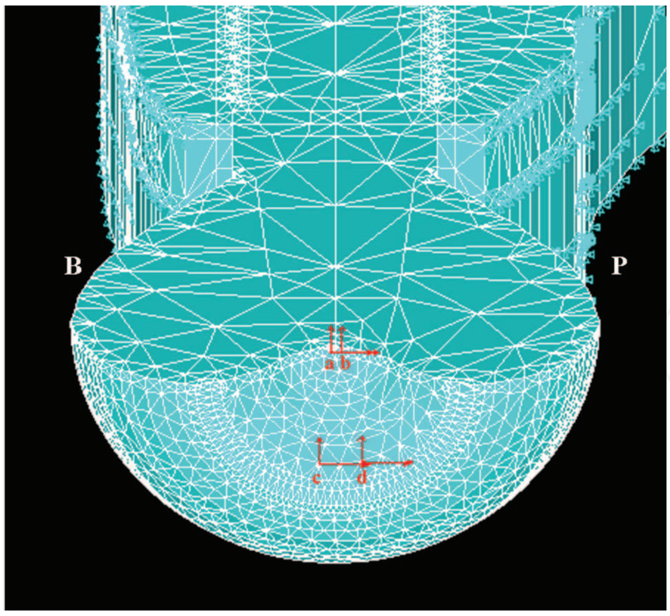


Fig. 9. Because a symmetric half model was used, loading was simulated by applying an oblique load (vertical load of 100 N and horizontal load of 20 N) from buccal to palatal at four different locations on the central (a, b) and distal fossa (c, d) of the crown.

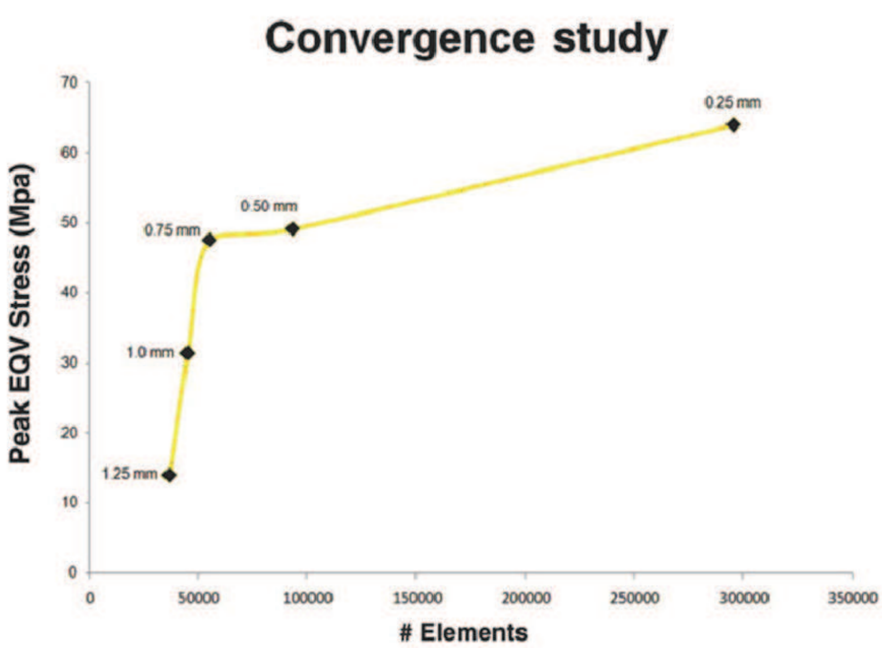


Fig. 10. Influence of element size (1.25, 1.0, 0.75, 0.50, and 0.25 mm) on bone mesh density and peak equivalent (EQV) stress in bone model (Courtesy from Pessoa RS et al. Clin Implant Dent Relat Res 2009).

| Study | Compact bone E (Gpa) | Poisson's ratio (v) | Cancellous bone E (Gpa) | Poisson's ratio (v) |
|---|---|---|---|---|
| Geng et al[37] | 13.4 | 0.3 | 1.37 | 0.31 |
| Borchers and Reichart[38] | 13.7 | 0.3 | 1.37 | 0.3 |
| Meijer et al[39] | 13.7 | 0.3 | 1.37 | 0.3 |
| Menicucci et al[40] | 13.7 | 0.3 | 1.37 | 0.3 |
| Teixeira et al[41] | 13.7 | 0.3 | 1.37 | 0.3 |
| Benzing et al[42] | 15 | 0.25 | 2 | 0.495 |
| Stegaroiu et al[43] | 15 | 0.3 | 1.5 | 0.3 |
| Ciftci and Canay[44] | 14 | 0.3 | 1 | 0.3 |
| Siegele and Soltesz[45] | 20 | 0.3 | 2 | 0.3 |
| Canay et al[46] | 19.73 | 0.3 | | |
| Geng et al[47] | 13.4 | 0.3 | 1.37 | 0.31 |
| | 10 | 0.3 | 1.37 | 0.31 |
| | 7.5 | 0.3 | 1.37 | 0.31 |
| | 5 | 0.3 | 1.37 | 0.31 |
| | 1.37 | 0.3 | 1.37 | 0.31 |

Table 1. Young's modulus (E) and Poisson's ratio (v) of compact and cancellous bone used in previous FEA studies.

| Material | Young's modulus E (Mpa) | | Poisson's ratio (v) | | Shear modulus G (Mpa) | |
|---|---|---|---|---|---|---|
| compact bone | Ex | 12,600 | vxy | 0.300 | | |
| | | | vyz | 0.253 | Gxy | 4,850 |
| | Ey | 12,600 | vxz | 0.253 | | |
| | | | vyx | 0.300 | Gyz | 5,700 |
| | Ez | 19,400 | vzy | 0.390 | | |
| | | | vzx | 0.390 | Gxz | 5,700 |
| cancellous bone | Ex | 1,148 | vxy | 0.055 | | |
| | | | vyz | 0.010 | Gxy | 68 |
| | Ey | 210 | vxz | 0.322 | | |
| | | | vyx | 0.010 | Gyz | 68 |
| | Ez | 1,148 | vzy | 0.055 | | |
| | | | vzx | 0.322 | Gxz | 434 |

Table 2. Material properties used in the transversely isotropic model (Courtesy from Huang HL et al. Clin Oral Implants Res 2005).

| | $E_y$ | $E_x$ | $E_z$ | $G_{yx}$ | $G_{yz}$ | $G_{xz}$ | $v_{yx}$ | $v_{yz}$ | $v_{xz}$ |
|---|---|---|---|---|---|---|---|---|---|
| Com. | 12.5 | 17.9 | 26.6 | 4.5 | 5.3 | 7.1 | 0.18 | 0.31 | 0.28 |
| Can. | 0.21 | 1.148 | 1.148 | 0.068 | 0.068 | 0.434 | 0.055 | 0.055 | 0.322 |

Table 3. Anisotropy elastic coefficients for compact (Com.)and cancellous (Can.) bone.

# Ei represents Young's modulus (GPa); Gij represents shear modulus (GPa); vij represents Poisson's ratio.

* The y-direction is infero-superior, the x-direction is medial-lateral, and the z-direction is anterior-posterior (Courtesy from Chang CL et al. Int J Oral Maxillofac Implants 2010).

## 12. References

Assuncao WG, Gomes EA, Barao VA, de Sousa EA. Stress analysis in simulation models with or without implant threads representation. Int J Oral Maxillofac Implants 2009;24:1040-1044.

Akca K, Iplikcioglu H. Evaluation of the effect of the residual bone angulation on implant-supported fixed prosthesis in mandibular posterior edentulism. Part II: 3-D finite element stress analysis. Implant Dent 2001;10:238-245.

Baggi L, Cappelloni I, Di Girolamo M, Maceri F, Vairo G. The influence of implant diameter and length on stress distribution of osseointegrated implants related to crestal bone geometry: a three-dimensional finite element analysis. J Prosthet Dent 2008;100:422-431.

Bell GH, Dunbar O, Beck JS, Gibb A. Variations in strength of vertebrae with age and their relation to osteoporosis. Calcif Tissue Res 1967;1:75-86

Benzing UR, Gall H, Weber H. Biomechanical aspects of two different implant-prosthetic concepts for edentulous maxillae. Int J Oral Maxillofac Implants 1995;10:188-198.

Bidez MW, Misch CE. Force transfer in implant dentistry: basic concepts and principles. J Oral Implantol 1992;18:264-274.

Borchers L, Reichart P. Three-dimensional stress distribution around a dental implant at different stages of interface development. J Dent Res 1983;62:155-159.

Branemark PI, Adell R, Breine U, Hansson BO, Lindstrom J, Ohlsson A. Intra-osseous anchorage of dental prostheses. I. Experimental studies. Scand J Plast Reconstr Surg 1969;3:81-100.

Branemark PI, Zarb GA, Albrektsson T (eds). Tissue-integrated prostheses: Osseointegration in clinical dentistry. Chicago: Quintessence, 1985:129.

Brosh T, Pilo R, Sudai D. The influence of abutment angulation on strains and stresses along the implant/bone interface: comparison between two experimental techniques. J Prosthet Dent 1998;79:328-334.

Caglar A, Aydin C, Ozen J, Yilmaz C, Korkmaz T. Effects of mesiodistal inclination of implants on stress distribution in implant-supported fixed prostheses. Int J Oral Maxillofac Implants 2006;21:36-44.

Canay S, Hersek N, Akpinar I, Asik Z. Comparison of stress distribution around vertical and angled implants with finite-element analysis. Quintessence Int 1996;27:591-598.

Chang CL, Chen CS, Hsu ML. Biomechanical effect of platform switching in implant dentistry: a three-dimensional finite element analysis. Int J Oral Maxillofac Implants 2010;25:295-304.
Chun HJ, Shin HS, Han CH, Lee SH. Influence of implant abutment type on stress distribution in bone under various loading conditions using finite element analysis. Int J Oral Maxillofac Implants 2006;21:195-202.
Ciftci Y, Canay S. Stress distribution on the metal framework of the implant-supported fixed prosthesis using different veneering materials. Int J Prosthodont 2001;14:406-411.
Clelland NL, Lee JK, Bimbenet OC, Brantley WA. A three-dimensional finite element stress analysis of angled abutments for an implant placed in the anterior maxilla. J Prosthodont 1995;4:95-100.
Cowin SC. Bone mechanics handbook. 2nd ed. Boca Raton (FL): CRC Press;2001. p. 1.1-1.23.
Cruz M, Wassall T, Toledo EM, Barra LP, Lemonge AC. Three-dimensional finite element stress analysis of a cuneiform-geometry implant. Int J Oral Maxillofac Implants 2003;18:675-684.
Dalkiz M, Zor M, Aykul H, Toparli M, Aksoy S. The three-dimensional finite element analysis of fixed bridge restoration supported by the combination of teeth and osseointegrated implants. Implant Dent 2002;11:293-300.
Ding X, Liao SH, Zhu XH, Zhang XH, Zhang L. Effect of diameter and length on stress distribution of the alveolar crest around immediate loading implants. Clin Implant Dent Relat Res 2009;11:279-287.
Ding X, Zhu XH, Liao SH, Zhang XH, Chen H. Implant-bone interface stress distribution in immediately loaded implants of different diameters: a three-dimensional finite element analysis. J Prosthodont 2009;18:393-402.
Eckert SE, Choi YG, Sanchez AR, Koka S. Comparison of dental implant systems: quality of clinical evidence and prediction of 5-year survival. Int J Oral Maxillofac Implants 2005;20:406-415.
Ferrigno N, Laureti M, Fanali S, Grippaudo G. A long-term follow-up study of non-submerged ITI implants in the treatment of totally edentulous jaws. Part I: Ten-year life table analysis of a prospective multicenter study with 1286 implants. Clin Oral Implants Res 2002;13:260-273.
Geng JP, Tan KB, Liu GR. Application of finite element analysis in implant dentistry: a review of the literature. J Prosthet Dent 2001;85:585-598.
Geng JP, Ma QS, Xu W, Tan KB, Liu GR. Finite element analysis of four thread-form configurations in a stepped screw implant. J Oral Rehabil 2004;31:233-239.
Geng JP, Xu DW, Tan KB, Liu GR. Finite element analysis of an osseointegrated stepped screw dental implant. J Oral Implantol 2004;30:223-233.
Hagberg C. Assessment of bite force: a review. J Craniomandib Disord 1987;1:162-169.
Heckmann SM, Karl M, Wichmann MG, Winter W, Graef F, Taylor TD. Loading of bone surrounding implants through three-unit fixed partial denture fixation: a finite-element analysis based on in vitro and in vivo strain measurements. Clin Oral Implants Res 2006;17:345-350.
Holmgren EP, Seckinger RJ, Kilgren LM, Mante F. Evaluating parameters of osseointegrated dental implants using finite element analysis--a two-dimensional comparative study examining the effects of implant diameter, implant shape, and load direction. J Oral Implantol 1998;24:80-88.

Hsu JT, Fuh LJ, Lin DJ, Shen YW, Huang HL. Bone strain and interfacial sliding analyses of platform switching and implant diameter on an immediately loaded implant: experimental and three-dimensional finite element analyses. J Periodontol 2009;80:1125-1132.

Hsu ML, Chen FC, Kao HC, Cheng CK. Influence of off-axis loading of an anterior maxillary implant: a 3-dimensional finite element analysis. Int J Oral Maxillofac Implants 2007;22:301-309.

Hsu ML, Chen CS, Chen BJ, Huang HH, Chang CL. Effects of post materials and length on the stress distribution of endodontically treated maxillary central incisors: a 3D finite element analysis. J Oral Rehabil 2009;36:821-830.

Huang HL, Huang JS, Ko CC, Hsu JT, Chang CH, Chen MY. Effects of splinted prosthesis supported a wide implant or two implants: a three-dimensional finite element analysis. Clin Oral Implants Res 2005;16:466-472.

Huang HL, Chang CH, Hsu JT, Fallgatter AM, Ko CC. Comparison of implant body designs and threaded designs of dental implants: a 3-dimensional finite element analysis. Int J Oral Maxillofac Implants 2007;22:551-562.

Juodzbalys G, Kubilius R, Eidukynas V, Raustia AM. Stress distribution in bone: single-unit implant prostheses veneered with porcelain or a new composite material. Implant Dent 2005;14:166-175.

Kao HC, Gung YW, Chung TF, Hsu ML. The influence of abutment angulation on micromotion level for immediately loaded dental implants: a 3-D finite element analysis. Int J Oral Maxillofac Implants 2008;23:623-630.

Kitamura E, Stegaroiu R, Nomura S, Miyakawa O. Biomechanical aspects of marginal bone resorption around osseointegrated implants: considerations based on a three-dimensional finite element analysis. Clin Oral Implants Res 2004;15:401-412.

Kong L, Hu K, Li D, Song Y, Yang J, Wu Z, et al. Evaluation of the cylinder implant thread height and width: a 3-dimensional finite element analysis. Int J Oral Maxillofac Implants 2008;23:65-74.

Kong L, Gu Z, Li T, Wu J, Hu K, Liu Y, et al. Biomechanical optimization of implant diameter and length for immediate loading: a nonlinear finite element analysis. Int J Prosthodont 2009;22:607-615.

Liao SH, Tong RF, Dong JX. Influence of anisotropy on peri-implant stress and strain in complete mandible model from CT. Comput Med Imaging Graph 2008;32:53-60.

Li T, Kong L, Wang Y, Hu K, Song L, Liu B, et al. Selection of optimal dental implant diameter and length in type IV bone: a three-dimensional finite element analysis. Int J Oral Maxillofac Surg 2009;38:1077-1083.

Lin CL, Chang SH, Wang JC, Chang WJ. Mechanical interactions of an implant/tooth-supported system under different periodontal supports and number of splinted teeth with rigid and non-rigid connections. J Dent 2006;34:682-691.

Lin CL, Wang JC, Ramp LC, Liu PR. Biomechanical response of implant systems placed in the maxillary posterior region under various conditions of angulation, bone density, and loading. Int J Oral Maxillofac Implants 2008;23:57-64.

Maeda Y, Miura J, Taki I, Sogo M. Biomechanical analysis on platform switching: is there any biomechanical rationale? Clin Oral Implants Res 2007;18:581-584.

Meijer GJ, Starmans FJ, de Putter C, van Blitterswijk CA. The influence of a flexible coating on the bone stress around dental implants. J Oral Rehabil 1995;22:105-111.

Menicucci G, Lorenzetti M, Pera P, Preti G. Mandibular implant-retained overdenture: finite element analysis of two anchorage systems. Int J Oral Maxillofac Implants 1998;13:369-376.

Mellal A, Wiskott HW, Botsis J, Scherrer SS, Belser UC. Stimulating effect of implant loading on surrounding bone. Comparison of three numerical models and validation by in vivo data. Clin Oral Implants Res 2004;15:239-248.

Morneburg TR, Proschel PA. Measurement of masticatory forces and implant loads: a methodologic clinical study. Int J Prosthodont 2002;15:20-27.

Morneburg TR, Proschel PA. In vivo forces on implants influenced by occlusal scheme and food consistency. Int J Prosthodont 2003;16:481-486.

Nagasao T, Kobayashi M, Tsuchiya Y, Kaneko T, Nakajima T. Finite element analysis of the stresses around endosseous implants in various reconstructed mandibular models. J Craniomaxillofac Surg 2002;30:170-177.

Nagasao T, Kobayashi M, Tsuchiya Y, Kaneko T, Nakajima T. Finite element analysis of the stresses around fixtures in various reconstructed mandibular models--part II (effect of horizontal load). J Craniomaxillofac Surg 2003;31:168-175.

Natali AN, Pavan PG, Ruggero AL. Analysis of bone-implant interaction phenomena by using a numerical approach. Clin Oral Implants Res 2006;17:67-74.

Nomura T, Powers MP, Katz JL, Saito C. Finite element analysis of a transmandibular implant. J Biomed Mater Res B Appl Biomater 2007;80:370-376.

O'Mahony AM, Williams JL, Katz JO, Spencer P. Anisotropic elastic properties of cancellous bone from a human edentulous mandible. Clin Oral Implants Res 2000;11:415-421.

O'Mahony AM, Williams JL, Spencer P. Anisotropic elasticity of cortical and cancellous bone in the posterior mandible increases peri-implant stress and strain under oblique loading. Clin Oral Implants Res 2001;12:648-657.

Perry J, Lenchewski E. Clinical performance and 5-year retrospective evaluation of Frialit-2 implants. Int J Oral Maxillofac Implants 2004;19:887-891.

Pessoa RS, Muraru L, Junior EM, Vaz LG, Sloten JV, Duyck J, et al. Influence of Implant Connection Type on the Biomechanical Environment of Immediately Placed Implants - CT-Based Nonlinear, Three-Dimensional Finite Element Analysis. Clin Implant Dent Relat Res 2009.

Petrie CS, Williams JL. Comparative evaluation of implant designs: influence of diameter, length, and taper on strains in the alveolar crest. A three-dimensional finite-element analysis. Clin Oral Implants Res 2005;16:486-494.

Petrie CS, Williams JL. Probabilistic analysis of peri-implant strain predictions as influenced by uncertainties in bone properties and occlusal forces. Clin Oral Implants Res 2007;18:611-619.

Pierrisnard L, Hure G, Barquins M, Chappard D. Two dental implants designed for immediate loading: a finite element analysis. Int J Oral Maxillofac Implants 2002;17:353-362.

Rho JY, Ashman RB, Turner CH. Young's modulus of trabecular and cortical bone material: ultrasonic and microtensile measurements. J Biomech 1993;26:111-119.

Rieger MR, Mayberry M, Brose MO. Finite element analysis of six endosseous implants. J Prosthet Dent 1990;63:671-676.

Rosenberg ES, Torosian JP, Slots J. Microbial differences in 2 clinically distinct types of failures of osseointegrated implants. Clin Oral Implants Res 1991;2:135-144.

Saab XE, Griggs JA, Powers JM, Engelmeier RL. Effect of abutment angulation on the strain on the bone around an implant in the anterior maxilla: a finite element study. J Prosthet Dent 2007;97:85-92.

Sahin S, Cehreli MC, Yalcin E. The influence of functional forces on the biomechanics of implant-supported prostheses--a review. J Dent 2002;30:271-282.

Satoh T, Maeda Y, Komiyama Y. Biomechanical rationale for intentionally inclined implants in the posterior mandible using 3D finite element analysis. Int J Oral Maxillofac Implants 2005;20:533-539.

Schrotenboer J, Tsao YP, Kinariwala V, Wang HL. Effect of microthreads and platform switching on crestal bone stress levels: a finite element analysis. J Periodontol 2008;79:2166-2172.

Schwartz-Dabney CL, Dechow PC. Edentulation alters material properties of cortical bone in the human mandible. J Dent Res 2002;81:613-617.

Schwartz-Dabney CL, Dechow PC. Variations in cortical material properties throughout the human dentate mandible. Am J Phys Anthropol 2003;120:252-277.

Sekine H, Komiyama Y, Hotta H, Yoshida Y. Mobility characteristics and tactile sensitivity of osseointegrated fixture-supporting systems. In: van Steenberghe D (ed). Tissue integration in Oral Maxillofacial Reconstruction. Amsterdam: Elsevier, 1986:306-332.

Sertgoz A. Finite element analysis study of the effect of superstructure material on stress distribution in an implant-supported fixed prosthesis. Int J Prosthodont 1997;10:19-27.

Sevimay M, Turhan F, Kilicarslan MA, Eskitascioglu G. Three-dimensional finite element analysis of the effect of different bone quality on stress distribution in an implant-supported crown. J Prosthet Dent 2005;93:227-234.

Shi L, Li H, Fok AS, Ucer C, Devlin H, Horner K. Shape optimization of dental implants. Int J Oral Maxillofac Implants 2007;22:911-920.

Siegele D, Soltesz U. Numerical investigations of the influence of implant shape on stress distribution in the jaw bone. Int J Oral Maxillofac Implants 1989;4:333-340.

Stegaroiu R, Sato T, Kusakari H, Miyakawa O. Influence of restoration type on stress distribution in bone around implants: a three-dimensional finite element analysis. Int J Oral Maxillofac Implants 1998;13:82-90.

Tada S, Stegaroiu R, Kitamura E, Miyakawa O, Kusakari H. Influence of implant design and bone quality on stress/strain distribution in bone around implants: a 3-dimensional finite element analysis. Int J Oral Maxillofac Implants 2003;18:357-368.

Teixeira ER, Sato Y, Akagawa Y, Shindoi N. A comparative evaluation of mandibular finite element models with different lengths and elements for implant biomechanics. J Oral Rehabil 1998;25:299-303.

Tie Y, Wang DM, Ji T, Wang CT, Zhang CP. Three-dimensional finite-element analysis investigating the biomechanical effects of human mandibular reconstruction with autogenous bone grafts. J Craniomaxillofac Surg 2006;34:290-298.

Tonetti MS. Determination of the success and failure of root-form osseointegrated dental implants. Adv Dent Res 1999;13:173-180.

Van Oosterwyck H, Duyck J, Vander Sloten J, Van der Perre G, De Cooman M, Lievens S, et al. The influence of bone mechanical properties and implant fixation upon bone loading around oral implants. Clin Oral Implants Res 1998;9:407-418.

Van Oosterwyck H, Duyck J, Vander Sloten J, Van Der Perre G, Naert I. Peri-implant bone tissue strains in cases of dehiscence: a finite element study. Clin Oral Implants Res 2002;13:327-333.

Wakabayashi N, Ona M, Suzuki T, Igarashi Y. Nonlinear finite element analyses: advances and challenges in dental applications. J Dent 2008;36:463-471.

Waltimo A, Kemppainen P, Kononen M. Maximal contraction force and endurance of human jaw-closing muscles in isometric clenching. Scand J Dent Res 1993;101:416-421.

Waltimo A, Kononen M. Bite force on single as opposed to all maxillary front teeth. Scand J Dent Res 1994;102:372-375.

Yang J, Xiang HJ. A three-dimensional finite element study on the biomechanical behavior of an FGBM dental implant in surrounding bone. J Biomech 2007;40:2377-2385.

Zampelis A, Rangert B, Heijl L. Tilting of splinted implants for improved prosthodontic support: a two-dimensional finite element analysis. J Prosthet Dent 2007;97:S35-43.

Zarone F, Apicella A, Nicolais L, Aversa R, Sorrentino R. Mandibular flexure and stress build-up in mandibular full-arch fixed prostheses supported by osseointegrated implants. Clin Oral Implants Res 2003;14:103-114.


**Finite Element Analysis**

Edited by David Moratal

ISBN 978-953-307-123-7

Hard cover, 688 pages

**Publisher** Sciyo

**Published online** 17, August, 2010

**Published in print edition** August, 2010

Finite element analysis is an engineering method for the numerical analysis of complex structures. This book provides a bird's eye view on this very broad matter through 27 original and innovative research studies exhibiting various investigation directions. Through its chapters the reader will have access to works related to Biomedical Engineering, Materials Engineering, Process Analysis and Civil Engineering. The text is addressed not only to researchers, but also to professional engineers, engineering lecturers and students seeking to gain a better understanding of where Finite Element Analysis stands today.